

THE POWER SPECTRUM OF CLUSTERS OF GALAXIES AND THE PRESS-SCHECHTER APPROXIMATION

MIRT GRAMANN AND IVAN SUHHONENKO

Tartu Astrophysical Observatory, Tõravere EE-2444, Estonia

ABSTRACT

We examine the power spectrum of clusters in the Press-Schechter (PS) theory and in N-body simulations to see how the power spectrum of clusters is related to the power spectrum of matter density fluctuations in the Universe. An analytic model for the power spectrum of clusters for their given number density is presented, both for real space and redshift space. We test this model against results from N-body simulations and find that the agreement between the analytic theory and the numerical results is good for wavelengths $\lambda > 60h^{-1}$ Mpc. On smaller scales non-linear processes that are not considered in the linear PS approximation influence the result. We also use our analytic model to study the redshift-space power spectrum of clusters in cold dark matter models with a cosmological constant (Λ CDM) and with a scale-invariant Harrison-Zel'dovich initial spectrum of density fluctuations. We find that power spectra of clusters in these models are not consistent with the observed power spectra of the APM and Abell-ACO clusters. One possible explanation for the observed power spectra of clusters is an inflationary scenario with a scalar field with the potential that has a localized steplike feature. We use the PS theory to examine the power spectrum of clusters in this model.

Subject headings: methods: numerical –galaxies: clustering – galaxies: clusters: general – cosmology: theory – large scale structure of universe

1. INTRODUCTION

Clusters of galaxies are efficient tracers of the large-scale structure of the universe. A strong spatial correlation of clusters of galaxies (Bahcall & Soneira 1983; Klypin & Kopylov 1983) provided some of the first evidence for the existence of organized structure on large scales. To date, much effort has been devoted to determine the correlation function and the power spectrum of clusters of galaxies on large spatial scales (e.g. Postman, Huchra

& Geller 1992; Peacock & West 1992; Einasto et al. 1993; Dalton et al. 1994; Romer et al. 1994; Croft et al. 1997; Einasto et al. 1997a; Retzlaff et al. 1998; Tadros, Efstathiou & Dalton 1998). Figure 1 shows the power spectrum of the spatial distribution of the Abell-ACO clusters as determined by Einasto et al. (1999), and the power spectrum of the APM clusters as found by Tadros, Efstathiou & Dalton (1998). For comparison, we show in Figure 1 the power spectrum derived from the distribution of galaxies in the APM survey (Baugh & Efstathiou 1993). Observations give the power spectrum of clusters for a given number density of clusters, n_{cl} . The number density of the APM clusters and Abell clusters is $n_{cl} \sim 3.4 \times 10^{-5} h^3 \text{ Mpc}^{-3}$ and $n_{cl} \sim 2.5 \times 10^{-5} h^3 \text{ Mpc}^{-3}$, respectively (Dalton et al. 1994; Einasto et al. 1997b; Retzlaff et al. 1998).

As the observational data on the power spectrum of clusters improve, the need for precise theoretical predictions becomes increasingly important. The power spectrum of clusters for different cosmological models can be calculated using N-body simulations (e.g. Retzlaff et al. 1998; Tadros, Efstathiou & Dalton 1998; Suhhonenko & Gramann 1999). However, this approach is difficult as it requires simulations with a very large dynamical range to identify correctly a sufficient number of clusters. In this situation it would be useful to have an analytical approach to describe the origin of the power spectrum of clusters of galaxies and to predict it.

The correlation function of clusters of galaxies has been a subject of many attempts at analytical modelling (e.g. Kaiser 1984; Kashlinsky 1987; Cole & Kaiser 1989; Mann, Heavens, & Peacock 1993; Mo & White 1996, hereafter MW96; Catelan et al. 1998; Kashlinsky 1998). In particular, using the Press-Schechter (PS) formalism to calculate the correlation function of clusters in Lagrangian space and mapping from Lagrangian space to Eulerian space within the context of the spherical collapse model, MW96 have derived an analytical expression for the correlation function of clusters of mass M as

$$\xi_M(r) = b^2(M) \xi(r), \quad (1)$$

where $\xi(r)$ is the correlation function of matter density fluctuations. The bias parameter $b(M)$ is

$$b(M) = 1 + \frac{1}{\delta_t} \left(\frac{\delta_t^2}{\sigma^2(M)} - 1 \right), \quad (2)$$

where $\sigma^2(M)$ is the density dispersion on a mass scale M and $\delta_t = 1.686$. This equation has been found to be in good agreement with N-body results by MW96 and by Mo et al. (1996).

The power spectrum and the correlation function of clusters form a Fourier transform pair. Therefore, in the linear approximation the power spectrum of clusters of mass M can

be expressed as

$$P_M(k) = b^2(M) P(k), \quad (3)$$

where $P(k)$ is the power spectrum of matter density fluctuations.

In this paper we develop further the results obtained by MW96 and calculate the power spectrum and the correlation function of galaxy clusters for a given number density of clusters n_{cl} in Lagrangian space and in Eulerian space (eq. [15,23-24] and [25-27] below). Observations provide the distribution of clusters in redshift space, which is distorted due to peculiar velocities of clusters. In order to study the power spectrum of clusters in redshift space, we use the linear approximation derived by Kaiser (1987). In §3 we examine the cluster power spectrum in real space and in redshift space using N-body simulations with realistic initial power spectra and show that in both cases the PS theory gives an accurate description of the power spectrum of clusters at wavenumbers $k < 0.1h \text{ Mpc}^{-1}$ (or at wavelengths $\lambda > 60h^{-1} \text{ Mpc}$). In §4 we use our model to study the redshift-space power spectrum of clusters in different cold dark matter models. We study inflationary models with a scale-invariant initial spectrum of density fluctuations and with a steplike initial spectrum derived by Starobinsky (1992). §5 summarizes the main results.

A Hubble constant of $H_0 = 100h \text{ km s}^{-1} \text{ Mpc}^{-1}$ is used throughout this paper.

2. THE POWER SPECTRUM OF CLUSTERS IN THE PS APPROXIMATION

An important aspect of the PS model is that, being entirely based on linear theory, suitably extrapolated to the collapse time of spherical perturbations, it is, by definition, local in Lagrangian space. While this Lagrangian aspect of the theory does not have immediate implications for the study of the mass function of clusters of galaxies, it is important for the study of their spatial clustering properties.

Let us assume that the density contrast $\epsilon_M(\mathbf{q})$ on a mass scale M is a Gaussian random field. Here \mathbf{q} represents the comoving Lagrangian coordinate. The probability that one would find a density contrast between ϵ_M and $\epsilon_M + d\epsilon_M$ is

$$p(\epsilon_M) d\epsilon_M = \frac{1}{\sqrt{2\pi}\sigma(M)} \exp\left[-\frac{\epsilon_M^2}{2\sigma^2(M)}\right] d\epsilon_M. \quad (4)$$

The density dispersion $\sigma^2(M)$ can be written as

$$\sigma^2(M) \equiv \langle \epsilon_M^2 \rangle = \frac{1}{2\pi^2} \int P(k) W^2(kR) k^2 dk, \quad (5)$$

where $W(kR)$ is the Fourier transform of the window function applied to determine the density field. In this paper we will use the top-hat window function. For the top-hat window, the mass M is related to the window radius R as $M = 4\pi\rho_b R^3/3$ (where ρ_b is the mean background density).

Press & Schechter (1974) suggested that we can determine the probability that a cluster of mass M has formed as

$$\Pi_M = \int_{\delta_t}^{\infty} p(\epsilon_M) d\epsilon_M = \frac{1}{2} \operatorname{erfc} \left[\frac{\delta_t}{\sqrt{2}\sigma(M)} \right], \quad (6)$$

where δ_t is a certain threshold value. PS used a value $\delta_t = 1.686$, which is motivated by the spherical collapse model. The number density of clusters with the mass between M and $M + dM$ is given by (Press & Schechter 1974)

$$n(M)dM = 2 \frac{\rho_b}{M} \frac{d\Pi_M}{dM} dM = -\sqrt{\frac{2}{\pi}} \frac{\rho_b}{M} \frac{\delta_t}{\sigma^2(M)} \frac{d\sigma(M)}{dM} \exp \left[-\frac{\delta_t^2}{2\sigma^2(M)} \right] dM. \quad (7)$$

Equation (7) involves an additional correction factor 2 to allow all the matter in the universe to form bound structures (see Peacock & Heavens 1990; Bond et al. 1991 for a more detailed discussion of this correction). Therefore, the number density of clusters of mass larger than M can be expressed as

$$n_{cl>(> M) = \int_M^{\infty} n(M')dM' = -\frac{3}{(2\pi)^{3/2}} \int_R^{\infty} \frac{\delta_t}{\sigma^2(r)} \frac{d\sigma(r)}{dr} \exp \left[-\frac{\delta_t^2}{2\sigma^2(r)} \right] \frac{dr}{r^3}. \quad (8)$$

Equation (8) has been frequently used to determine the cluster abundance in different cosmological models (e.g. Efstathiou et al. 1988; White, Efstathiou & Frenk 1993; Lacey & Cole 1994; Eke, Cole & Frenk 1996; Borgani et al. 1997).

For a two-dimensional Gaussian distribution the probability density for finding simultaneously ϵ_{M_1} on scale M_1 and ϵ_{M_2} on scale M_2 separated by q is given by

$$p(\epsilon_{M_1}, \epsilon_{M_2}) = \frac{1}{2\pi\sigma(M_1)\sigma(M_2)\sqrt{1-\rho_{12}^2}} \exp \left[-\frac{1}{2(1-\rho_{12}^2)}(x_1^2 - 2\rho_{12}x_1x_2 + x_2^2) \right], \quad (9)$$

where $x_1 = \epsilon_{M_1}/\sigma(M_1)$, $x_2 = \epsilon_{M_2}/\sigma(M_2)$ and $\rho_{12} = \xi_{12}(q)/\sigma(M_1)\sigma(M_2)$ is the correlation coefficient between ϵ_{M_1} and ϵ_{M_2} . The $\xi_{12}(q)$ is the two-point correlation function of the linear density contrast smoothed on the scales M_1 and M_2 :

$$\xi_{12}(q) \equiv \langle \epsilon_{M_1}(\mathbf{q}_1)\epsilon_{M_2}(\mathbf{q}_2) \rangle = \frac{1}{2\pi^2} \int P(k) W(kR_1) W(kR_2) j_0(kq) k^2 dk, \quad (10)$$

where $q = |\mathbf{q}_1 - \mathbf{q}_2|$ and $j_0(x)$ is the spherical Bessel function of the order zero. Similarly to equation (6), we can write for the probability for two clusters of mass M_1, M_2 to form as

$$\Pi_{M_1 M_2} = \int_{\delta_t}^{\infty} \int_{\delta_t}^{\infty} p(\epsilon_{M_1}, \epsilon_{M_2}) d\epsilon_{M_1} d\epsilon_{M_2} . \quad (11)$$

To determine the correlation function of clusters of masses $[M_1; M_1 + dM_1]$ and $[M_2; M_2 + dM_2]$ we can use an expression

$$1 + \xi_{M_1 M_2}(q) = \frac{\frac{\partial^2 \Pi_{M_1 M_2}}{\partial M_1 \partial M_2}}{\frac{d\Pi_{M_1}}{dM_1} \frac{d\Pi_{M_2}}{dM_2}} . \quad (12)$$

A similar equation was used by Kashlinky (1987, 1998) to derive the correlation function of clusters in Eulerian space and by Catelan et al. (1998) to describe clustering in Lagrangian space.

In order to find the correlation function of clusters of mass larger than M , we start from approximations (6-7) and (11-12) and write down the probability to find two clusters in small volumes dV_1, dV_2 , one cluster being in the mass range $[M_1, M_1 + dM_1]$, the other in $[M_2, M_2 + dM_2]$, as

$$d\Phi(M_1, M_2) = 4 \frac{\rho_b^2}{M_1 M_2} \frac{\partial^2 \Pi_{M_1 M_2}}{\partial M_1 \partial M_2} dM_1 dM_2 dV_1 dV_2 . \quad (13)$$

We included in equation (13) a correction factor 4 to make it consistent with equation (7) at $\xi_{12}(q) = 0$. The probability to find two clusters of mass larger than M can be expressed as

$$d\Phi_{cl}(> M) = \int_M^{\infty} \int_M^{\infty} d\Phi(M_1, M_2) dM_1 dM_2 = n_{cl}^2 [1 + \xi_{cl}(q)] dV_1 dV_2 , \quad (14)$$

where n_{cl} is the number density of clusters of mass larger than M (equation 8). Therefore, the correlation function of clusters can be written in the form

$$1 + \xi_{cl}(q) = \frac{1}{n_{cl}^2} \int_M^{\infty} \int_M^{\infty} 4 \frac{\rho_b^2}{M_1 M_2} \frac{\partial^2 \Pi_{M_1 M_2}}{\partial M_1 \partial M_2} dM_1 dM_2 . \quad (15)$$

Equations (5,8-11) and (15) determine the correlation function of clusters for a given n_{cl} in the PS theory of gravitational clustering.

Let us consider the correlation function of clusters in the linear approximation, i.e. neglecting the terms involving $\xi_{12}^2(q)$ in equation (9). In the linear approximation, the probability density

$$p(\epsilon_{M_1}, \epsilon_{M_2}) = \frac{1}{2\pi\sigma(M_1)\sigma(M_2)} \left[1 + \frac{\xi_{12}(q)\epsilon_{M_1}\epsilon_{M_2}}{\sigma^2(M_1)\sigma^2(M_2)} \right] \exp \left[-\frac{\epsilon_{M_1}^2}{2\sigma^2(M_1)} \right] \exp \left[-\frac{\epsilon_{M_2}^2}{2\sigma^2(M_2)} \right] . \quad (16)$$

Substituting approximation (16) into equation (11) we find that

$$\Pi_{M_1 M_2} = \Pi_{M_1} \Pi_{M_2} + \frac{1}{2\pi} \frac{\xi_{12}(q)}{\sigma(M_1)\sigma(M_2)} \exp\left[-\frac{\delta_t^2}{2\sigma^2(M_1)}\right] \exp\left[-\frac{\delta_t^2}{2\sigma^2(M_2)}\right] \quad (17)$$

and

$$\frac{\partial^2 \Pi_{M_1 M_2}}{\partial M_1 \partial M_2} = \frac{d\Pi_{M_1}}{dM_1} \frac{d\Pi_{M_2}}{dM_2} \left[1 + \frac{\xi_{12}(q)}{\delta_t^2} \left(\frac{\delta_t^2}{\sigma^2(M_1)} - 1 \right) \left(\frac{\delta_t^2}{\sigma^2(M_2)} - 1 \right) \right]. \quad (18)$$

For separations q much larger than the smoothing lengths, $q \gg R_1$ and $q \gg R_2$, the influence of the window functions on the correlations is negligible, and the correlation function $\xi_{12}(q) \simeq \xi(q)$ (where $\xi(q)$ is the linear mass autocorrelation function). Therefore, in the linear approximation the correlation function of clusters of masses $[M_1; M_1 + dM_1]$ and $[M_2; M_2 + dM_2]$ can be written as

$$\xi_{M_1 M_2}(q) = b^L(M_1) b^L(M_2) \xi(q), \quad (19)$$

where the Lagrangian bias factor $b^L(M)$ is

$$b^L(M) = \frac{1}{\delta_t} \left(\frac{\delta_t^2}{\sigma^2(M)} - 1 \right). \quad (20)$$

MW96 derived this equation to describe clustering in Lagrangian space starting from the behaviour of the conditional Lagrangian mass function derived by Bond et al. (1991). By using the spherical collapse model, MW96 found that in Eulerian space the correlation function of clusters of masses $[M_1; M_1 + dM_1]$ and $[M_2; M_2 + dM_2]$ can be written as

$$\xi_{M_1 M_2}(r) = b(M_1) b(M_2) \xi(r), \quad (21)$$

where $\xi(r)$ is the correlation function of matter density fluctuations in Eulerian space and the Eulerian bias factor $b(M)$ is

$$b(M) = 1 + b^L(M) = 1 + \frac{1}{\delta_t} \left(\frac{\delta_t^2}{\sigma^2(M)} - 1 \right). \quad (22)$$

Catelan et al. (1998) used a more general method for evolving the spatial distribution of clusters and found a similar result for the linear approximation. The shift by 1 of the linear bias factor, caused here by the transformation from the Lagrangian to the Eulerian world, comes from mass conservation in Eulerian space.

Let us consider the correlation function of clusters for a given number density in the linear PS approximation. Substituting approximation (18) into equation (15) we find that in the linear approximation the Lagrangian correlation function of clusters for a given n_{cl} can be expressed as

$$\xi_{cl}(q) = (b_{cl}^L)^2 \xi(q), \quad (23)$$

where the bias parameter b_{cl}^L can be written in the form

$$b_{cl}^L = \frac{1}{n_{cl}} \int_M^\infty b^L(M') n(M') dM' = -\frac{3}{(2\pi)^{3/2} n_{cl}} \int_R^\infty \frac{1}{\sigma^2(r)} \frac{d\sigma(r)}{dr} \left[\frac{\delta_t^2}{\sigma^2(r)} - 1 \right] \exp \left[-\frac{\delta_t^2}{2\sigma^2(r)} \right] \frac{dr}{r^3}. \quad (24)$$

Similarly to equations (21-22) the Eulerian correlation function of clusters for a given number density n_{cl} can be written as

$$\xi_{cl}(r) = b_{cl}^2 \xi(r), \quad (25)$$

where the bias parameter b_{cl} is

$$b_{cl} = 1 + b_{cl}^L = 1 - \frac{3}{(2\pi)^{3/2} n_{cl}} \int_R^\infty \frac{1}{\sigma^2(r)} \frac{d\sigma(r)}{dr} \left[\frac{\delta_t^2}{\sigma^2(r)} - 1 \right] \exp \left[-\frac{\delta_t^2}{2\sigma^2(r)} \right] \frac{dr}{r^3}. \quad (26)$$

The power spectrum of clusters for a given number density in the linear approximation can be expressed as

$$P_{cl}(k) = b_{cl}^2 P(k). \quad (27)$$

The cluster bias parameter b_{cl} depends on the minimal mass M (or the window radius R) of clusters and on the power spectrum of density fluctuations, $P(k)$, which determines the function $\sigma(r)$. For a fixed $P(k)$ and n_{cl} , the minimal mass M (or scale R) can be determined by inverting equation (8). In this approach the power spectrum (or the correlation function) of clusters does not depend on the mean background density ρ_b (or the density parameter Ω_0).

Observations provide the distribution of clusters in redshift space, which is distorted due to peculiar velocities of clusters. On large scales, where linear theory applies, the power spectrum of matter density fluctuations in redshift space is given by (Kaiser 1987):

$$P^s(k) = \left[1 + \frac{2f(\Omega_0)}{3} + \frac{f^2(\Omega_0)}{5} \right] P(k), \quad (28)$$

where $f(\Omega_0) \approx \Omega_0^{0.6}$ is the linear velocity growth factor. In the linear approximation (27), relation (28) takes the form

$$P_{cl}^s(k) = \left[1 + \frac{2f(\Omega_0)}{3b_{cl}} + \frac{f^2(\Omega_0)}{5b_{cl}^2} \right] b_{cl}^2 P(k). \quad (29)$$

Equation (29) determines the power spectrum of clusters for a given n_{cl} in redshift space.

3. NUMERICAL RESULTS

For testing the solutions (26-27) and (29), we ran N-body simulations, using a particle-mesh code described by Gramann (1988). We investigated the evolution of 256^3 particles on a 256^3 grid, with $\Omega = 1$. The comoving box size was $L = 384h^{-1}$ Mpc. The initial density field was taken to be Gaussian.

We examined the distribution of clusters in two cosmological models which start from the observed power spectra of the distribution of galaxies and clusters of galaxies. In the model (1), the initial linear power spectrum of density fluctuations was chosen in the form $P(k) \propto k^{-2}$ at wavelengths $\lambda < 120h^{-1}$ Mpc. In the model (2), we assumed that the initial power spectrum contains a primordial feature at the wavelengths $\lambda \sim 30 - 60h^{-1}$ Mpc that correspond to the scale of superclusters of galaxies. Suhhonenko & Gramann (1998) studied the mass function, peculiar velocities, the power spectrum and the correlation function of clusters in both models for different values of the density parameter Ω_0 and σ_8 (the rms fluctuation on the $8h^{-1}$ Mpc scale). The results were compared with observations. They found that in many aspects the initial power spectrum of density fluctuations in the model (2) fits the observed data better than the simple power law model (1).

Clusters were selected in the simulations as maxima of the density field that was determined on a 256^3 grid using the CIC-scheme. To determine peculiar velocities of clusters, we determined the peculiar velocity field on a 256^3 grid using the CIC-scheme and found the peculiar velocities at the grid points where clusters had been identified. The clusters were then ranked according to their density and we selected $N_{cl} = (L/d_{cl})^3$ highest ranked clusters to produce cluster catalogs with a mean intercluster separation $d_{cl} = 30 - 40h^{-1}$ Mpc. For comparison, the mean separation of the observed APM and Abell clusters is $d_{cl} \sim 31h^{-1}$ and $d_{cl} \sim 34h^{-1}$ Mpc, respectively (Dalton et al. 1994; Retzlaff et al. 1998).

It is difficult to follow the evolution of rich clusters by using N-body simulations, as it requires simulations with a very large dynamical range to identify correctly a sufficient number of clusters. We determined clusters as maxima of the density field smoothed on the scale $R \sim 1.5h^{-1}$ Mpc. This method of identifying clusters is not really identical to that what the PS theory is predicting - the location of collapsed, virialized objects - and this could affect the degree of agreement between the analytic theory and the numerical results. However, in order to increase the resolution of simulations we must increase the number of test particles and grid points, or we have to follow the evolution of clusters in a smaller box. While the first possibility is technically difficult, in the latter case the number of rich clusters becomes too small to get statistically reliable results. Taking into account the requirements on the number of clusters and on the resolution together with the fact

of fixed computer resources we decided to use a box size $L = 384h^{-1}$ Mpc and a grid size $R_g = 1.5h^{-1}$ Mpc.

Figure 2 shows the power spectrum of clusters with a mean separation $d_{cl} = 30h^{-1}$ Mpc in our models. We studied also the power spectrum of clusters with a mean separation $d_{cl} = 35h^{-1}$ Mpc and $d_{cl} = 40h^{-1}$ Mpc, and found similar results. To calculate the power spectrum of clusters in the simulations we determined the density field of clusters on a 128^3 grid using the CIC-scheme and calculated its Fourier components, subtracting the shot noise term. We determined also the Poisson error bars for the power spectrum. In a shell of k -space containing m modes, the Poisson error can be estimated as $\Delta P_{cl}(k) = 2^{1/2} m^{-1/2} d_{cl}^3$ (see e.g. Peacock & Nicholson (1991) for a more detailed analysis of the Poisson errors in the power spectrum).

Figure 2a shows the results for the model (1) and Figure 2b for the model (2). For the model (1), the clusters were determined in the simulation for $\sigma_8 = 0.5$ and $\sigma_8 = 0.8$. For the model (2), these parameters were $\sigma_8 = 0.5$ and $\sigma_8 = 0.84$. For comparison, we examined the power spectrum of clusters in the linear PS approximation (27). We inverted equation (8) to determine the minimal radius R for a given n_{cl} (or d_{cl}) and after that we calculated the bias factor b_{cl} using equation (26). For a given σ_8 and n_{cl} , the bias parameter b_{cl} in the model (1) is similar to that in the model (2). For $\sigma_8 = 0.5$, we find that $b_{cl} = 4.3$ and 4.9 for separations $d_{cl} = 30$ and $40h^{-1}$ Mpc, respectively. For $\sigma_8 = 0.8$, $b_{cl} = 2.9$ and 3.3 , respectively.

Now we can compare the numerical results and the PS theory predictions. First, consider the power spectrum of clusters at wavenumbers $k = 0.04 - 0.1h$ Mpc $^{-1}$ (or at wavelengths $\lambda = 60 - 160h^{-1}$ Mpc). On larger scales, the number of modes in the simulations is too small to get statistically reliable results. Figure 2 demonstrates that at wavenumbers $k = 0.04 - 0.1h$ Mpc $^{-1}$, the power spectrum of clusters in the simulations is linearly enhanced with respect to the power spectrum of the matter distribution in both models studied. For $\sigma_8 = 0.5$, the agreement between the results of the N-body simulations and the PS theory predictions is very good. The mean deviation between the numerical results and the theoretical predictions is about 4% and 7% in the model (1) and in the model (2), respectively. For $\sigma_8 \approx 0.8$, we find that the power spectrum of clusters in N-body simulations is somewhat lower than predicted by approximation (27). The power spectrum of clusters is about 80% and 70% of the linear theory predictions in the model (1) and model (2), respectively. The PS approximation predicts that during the evolution between the $\sigma_8 = 0.5$ and $\sigma_8 = 0.8$, $P_{cl}(k)$ increases slightly. In simulations we find that during the evolution the power spectrum of clusters decreases. This effect is probably caused by merging of very rich clusters. Further study (e.g. numerical simulations with a higher

dynamical range) is needed to determine whether this is a real effect in our models, or a numerical effect due to the limited dynamical range of the N-body simulations.

Let us now consider the power spectrum of clusters at wavenumbers $k = 0.1 - 0.2h$ Mpc^{-1} ($\lambda = 30 - 60h^{-1}$ Mpc). In the model (1), the numerical results on these scales are in good agreement with the linear approximation (27). But in the model (2), the power spectrum of clusters in the simulation is significantly smaller than that predicted by the linear theory. For $\sigma_8 = 0.84$, we find that the power spectrum of clusters is only 30% of the linear theory predictions. Therefore, in the model (2), we cannot use the linear approximation to study the power spectrum of clusters at wavenumbers $k > 0.1h$ Mpc^{-1} . The power spectrum of clusters on these scales is probably determined by non-linear processes in superclusters of galaxies.

Figure 3 shows the redshift-space power spectrum of clusters in the simulations and in approximation (29). For clarity, we did not plot error bars in this Figure. In order to study peculiar velocities of galaxy clusters and their distribution in redshift space in models with different Ω_0 , we determined peculiar velocities of clusters in the simulations with $\Omega = 1$ and assumed that peculiar velocities of clusters are proportional to the linear growth factor $f(\Omega_0)$. Let us consider the redshift-space power spectrum of clusters at wavenumbers $k = 0.04 - 0.1h$ Mpc^{-1} , where we expect that the linear approximation (29) applies. Numerical results show that on these scales the power spectrum of clusters in redshift space is linearly enhanced with respect to the power spectrum of clusters in real space. In Figure 3 we show the power spectrum of clusters in redshift space for $\sigma_8 = 0.5$ and $\Omega = 1$. In this case, the agreement between the numerical results and approximation (29) is very good. The mean deviation between the numerical results and theoretical predictions is about 5% and 7%, in the model (1) and model (2), respectively. For $\sigma_8 \approx 0.8$ we find that, similarly to real space, the redshift-space power spectrum of clusters in the simulations is somewhat lower than that predicted by the linear theory. For $\Omega = 1$, the power spectrum of clusters is about 80% and 75% of the linear theory predictions in the model (1) and model (2), respectively. For $\Omega_0 = 0.2$, we found similar results. Within the uncertainties due to various numerical effects in the simulations, the agreement between the analytic theory and the numerical results is good. The degree of agreement is similar in real and in redshift space.

4. MODELS WITH COLD DARK MATTER

Now we use approximation (29) to analyze the redshift-space power spectrum of clusters in different cold dark matter models. We examine flat cosmological models with

the density parameter $\Omega_0 = 0.3 - 0.4$, the baryonic density $\Omega_B = 0.015h^{-2}$ and the normalized Hubble constant $h = 0.5 - 0.7$. These parameters are in agreement with recent nucleosynthesis results (Tytler et al. 1996), with measurements of the density parameter (e.g. Dekel, Burstein & White 1996; Bahcall & Fan 1998) and with measurements of the Hubble constant using various distance indicators (e.g. Tammann 1998). To restore the spatial flatness in the low-density models, we assume a contribution from a cosmological constant: $\Omega_\Lambda = 1 - \Omega_0$.

Figure 4 shows the redshift-space power spectrum of clusters in the Λ CDM models with a scale-invariant Harrison-Zel'dovich initial spectrum of density fluctuations ($P_{in}(k) \propto k$). We have used the transfer function derived by Bardeen et al. (1986) and Sugiyama (1995), and the COBE normalization derived by Bunn & White (1997). Figure 4a demonstrates the power spectrum of the model clusters and the Abell-ACO clusters with a mean separation $d_{cl} = 34h^{-1}$ Mpc. We show the power spectrum of the Abell-ACO clusters as found by Einasto et al. (1999). This spectrum represents the weighted mean of the power spectra determined by Einasto et al. (1997a) and Retzlaff et al. (1998). Einasto et al. (1997a) determined the power spectrum of the Abell-ACO clusters from the correlation function of clusters, while Retzlaff et al. (1998) estimated the power spectrum directly (see Einasto et al. 1999 for details). The power spectrum of the distribution of the Abell-ACO clusters peaks at the wavenumber $k = 0.052h$ Mpc $^{-1}$ (or at the wavelength $\lambda = 120h^{-1}$ Mpc). For $k > 0.052h$ Mpc $^{-1}$, the cluster power spectrum is well approximated by a power law, $P(k) \propto k^n$, with $n \approx -1.9$. A similar peak in the one-dimensional power spectrum of a deep pencil-beam survey was detected by Broadhurst et al. (1990) and in the two-dimensional power spectrum of the Las Campanas redshift survey by Landy et al. (1996). Figure 4b shows the power spectrum of the model clusters with a mean separation $d_{cl} = 31h^{-1}$ Mpc. For comparison, we show the power spectrum of the observed APM clusters determined by Tadros, Efstathiou & Dalton (1998). They analyzed the redshift survey of 364 clusters described by Dalton et al. (1994). The mean intercluster separation of APM clusters is $d_{cl} \sim 31h^{-1}$ Mpc (Dalton et al. 1994).

Figure 4 shows that the power spectrum of clusters predicted in the Λ CDM models is not consistent with the observed spectra of clusters. We studied a χ^2 probability at wavenumbers $k = 0.03 - 0.1h$ Mpc $^{-1}$, where we expect that the linear approximation (29) applies. For the models presented in Figure 4, the probability to fit the observed power spectra of the Abell and APM clusters is less than 5×10^{-2} and 10^{-6} , respectively. We also studied a χ^2 probability for the models, where the amplitude of the power spectrum of clusters is about 70% and 80% of the linear theory predictions and found similar results. The power spectrum of clusters in the Λ CDM models with a scale-invariant initial spectrum is not consistent with the observed spectra of the APM and Abell-ACO clusters (see also

e.g. Tadros, Efstathiou & Dalton 1998; Einasto et al. 1997a).

The power spectrum of density fluctuations in the universe depends on the physical processes in the early universe. The peak in the power spectrum of clusters at wavelength $\lambda \simeq 120h^{-1}$ Mpc may be generated during the era of radiation domination or earlier. Baryonic acoustic oscillations in adiabatic models may explain the observed power spectrum only if currently favored determinations of cosmological parameters are in substantial error (e.g. the density parameter $\Omega_0 < 0.2h$) (Eisenstein et al. 1998). One possible explanation for the observed power spectra of clusters is an inflationary model with a scalar field whose potential $V(\varphi)$ has a local steplike feature in the first derivative. This feature can be produced by fast phase transition in physical field other than an inflaton field. An exact analytical expression for the scalar (density) perturbations generated in this inflationary model was found by Starobinsky (1992) (see also Lesgourgues, Polarski & Starobinsky 1998). The initial power spectrum of density fluctuations in this model can be expressed as

$$P_{in}(k) \propto \frac{k S(k/k_0, p)}{p^2}, \quad (30)$$

where function $S(k/k_0, p)$ can be written in the form

$$S(y, p) = 1 - \frac{3p_1}{y} \left[f_1(y) \sin 2y + \frac{2}{y} \cos 2y \right] + \frac{9p_1^2 f_2(y)}{2y^2} \left[f_2(y) + f_1(y) \cos 2y - \frac{2}{y} \sin 2y \right]. \quad (31)$$

Here, function $f_1(y) = 1 - y^{-2}$, $f_2(y) = 1 + y^{-2}$ and $p_1 = p - 1$. The initial power spectrum in this model depends on two parameters k_0 and p . The parameter k_0 determines the location of the step and the parameter p - the shape of the initial spectrum. For $p = 1$, we recover the scale-invariant Harrison-Zel'dovich spectrum ($S(y, 1) \equiv 1$). At present, the initial spectrum (30-31) is probably the only example of a initial power spectrum with the desired properties, for which a closed analytical form exists.

Figure 5 shows the power spectrum of clusters in the Λ CDM models with a steplike initial power spectrum. As in Figure 4, we have used the transfer function derived by Bardeen et al. (1986) and Sugiyama (1995), and the COBE normalization derived by Bunn & White (1997). For the models with $p < 1$ and $p > 1$, the step parameter was chosen to be $k_0 = 0.016h$ Mpc $^{-1}$ and $k_0 = 0.03h$ Mpc $^{-1}$, respectively. In this case, in the models with $p < 1$, the power spectrum has a well-defined maximum at the wavenumber $k \simeq 0.05h$ Mpc $^{-1}$ and a second maximum at $k \simeq 0.1h$ Mpc $^{-1}$. In the models with $p > 1$, the picture is inverted. The power spectrum has a flat upper plateau at wavenumbers $k < 0.05h$ Mpc $^{-1}$, a sharp decrease on smaller scales ($k = 0.05 - 0.1h$ Mpc $^{-1}$) and a secondary maximum at $k \simeq 0.15h$ Mpc $^{-1}$. At wavenumbers $k > 0.05h$ Mpc $^{-1}$, the power spectrum in the Λ CDM models with $p \simeq 1.3 - 1.4$ is similar to the power spectrum in the numerical model (2), that we studied in §3 (see Figure 2b and Figure 3b).

Figure 5a shows the power spectrum of the model clusters and the Abell clusters with a mean separation $d_{cl} = 34h^{-1}$ Mpc. We have studied inflationary models with parameter $p = 0.6 - 0.8$. Figure 5a shows that the shape of the cluster power spectrum in these models is in good agreement with the observed power spectrum of the Abell-ACO clusters. However, the amplitude of the observed spectrum of clusters is about 70% lower than predicted in these models by using approximation (29). We found a similar effect in §3 by comparing the analytic and numerical results. It is possible that the linear approximation (29) somewhat overestimates the power spectrum of clusters due to dynamical effects that are not taken into account in this approximation. Therefore, the power spectrum of clusters can be expressed as

$$P_{cl}^s(k) = F \left[1 + \frac{2f(\Omega_0)}{3b_{cl}} + \frac{f^2(\Omega_0)}{5b_{cl}^2} \right] b_{cl}^2 P(k), \quad (32)$$

where the factor $F = 0.7 - 1.0$. For $F = 0.7$, the inflationary models studied in Figure 5a, are consistent with the power spectrum of the Abell-ACO clusters at a confidence level of $> 90\%$ (based on a χ^2 test at $k = 0.03 - 0.1h$ Mpc $^{-1}$). Figure 5b demonstrates the power spectrum of the model clusters and the APM clusters with a mean separation $d_{cl} = 31h^{-1}$ Mpc. We have studied the Λ CDM model with $p = 1.25$. For $F = 0.7$, the cluster power spectrum in this model is consistent with the observed power spectrum of the APM clusters at a confidence level of $> 50\%$. (For $F = 0.65$, at a confidence level of $> 90\%$).

Available data are insufficient to rule out any of the models studied in Figure 5. Note that the power spectra of clusters predicted in the models with $p < 1$ and $p > 1$ are rather different on large scales, where $k < 0.05h$ Mpc $^{-1}$. Therefore, accurate measurements of the power spectrum of clusters and galaxies on these scales can serve as a discriminating test for these interesting models.

5. SUMMARY AND CONCLUSIONS

Because of the low density of rich clusters of galaxies and their enhanced clustering strength compared to galaxies, rich clusters provide a powerful probe of large-scale structure in the Universe. In this paper, we have examined the power spectrum of clusters in the Press-Schechter (PS) theory and in N-body simulations to see how the power spectrum of clusters is related to the power spectrum of matter density fluctuations in the Universe. We have derived an analytical expression to determine the correlation function of clusters for a given number density of clusters in Lagrangian space and have examined this expression in the linear approximation. In order to study the power spectrum of clusters in redshift space, we used the approximation derived by Kaiser (1987).

For testing our analytic results, we used N-body simulations with realistic initial power spectra of density fluctuations. We investigated the power spectrum of clusters with a mean separation $d_{cl} = 30 - 40h^{-1}$ Mpc. The numerical results showed that we can use the linear PS approximation to predict the power spectrum of clusters in real space and in redshift space at wavenumbers $k < 0.1h^{-1}$ Mpc. On smaller scales non-linear processes that are not taken into account in the linear PS approximation influence the results.

We also used the PS approximation to analyze the redshift-space power spectrum of clusters in Λ CDM models. We investigated inflationary models with a scale-invariant initial spectrum of density fluctuations and with a steplike initial spectrum derived by Starobinsky (1992). The results were compared with observations. We found that the power spectrum of clusters in the Λ CDM models with a scale-invariant initial spectrum is not consistent with the observed spectra of the APM and Abell clusters. We investigated also inflationary models with a steplike initial power spectrum (30-31) that depends on two parameters k_0 and p . The parameter k_0 determines the location of the step and the parameter p - the shape of the initial spectrum. For the models with $p < 1$ and $p > 1$, the step parameter was chosen to be $k_0 = 0.016h$ Mpc $^{-1}$ and $k_0 = 0.03h$ Mpc $^{-1}$, respectively. We found that the power spectrum of clusters in these Λ CDM models is in good agreement with the observed power spectrum of the Abell-ACO clusters, if the initial parameter p is in the range $p = 0.6 - 0.8$. To describe the power spectrum of the APM clusters, we can use the Λ CDM model with parameter $p = 1.25$.

We thank J. Einasto, A. Kashlinsky, S. Matarrese, H. Mo and E. Saar for useful discussions. This work has been supported by the ESF grant 97-2645.

REFERENCES

- Bahcall, N. A., & Fan, X. 1998, Proc. Nat. Acad. Sci. USA, 95, 5956
- Bahcall, N. A., & Soneira, R. M. 1983, ApJ, 270, 20
- Bardeen, J. M., Bond, J. R., Kaiser, N., & Szalay, A. S. 1986, ApJ, 304, 15
- Baugh, C., & Efstathiou, G. 1993, MNRAS, 265, 145
- Bond, J. R., Cole, S., Efstathiou, G., & Kaiser, N. 1991, ApJ, 379, 440
- Borgani, S. et al. 1997, NewA, 1, 321
- Broadhurst, T.J., Ellis, R.S., Koo, D.S., & Szalay, A.S. 1990, Nature, 343, 726
- Bunn, E.F., & White, M. 1997, ApJ, 480, 6
- Dalton, G. B., Croft, R. A. C., Efstathiou, G., Sutherland, W. J., Maddox, S. J., & Davis, M. 1994, MNRAS, 271, L47
- Dekel, A., Burstein, D., & White, S. D. M. 1996, in Critical Dialogues in Cosmology, ed. Neil Turok, (Singapore:World Scientific)
- Catelan, P., Lucchin, F., Matarrese, S., & Porciani, C. 1998, MNRAS, 297, 692
- Cole, S., & Kaiser, N., 1989, MNRAS, 237, 1127
- Croft, R. A. C., Dalton, G. B., Efstathiou, G., Sutherland, W. J., & Maddox, S. J. 1997, MNRAS, 291, 305
- Efstathiou, G., Frenk, C.S., White, S.D.M., & Davis, M. 1988, MNRAS, 235, 715
- Einasto, J., Gramann, M., Saar E., & Tago, E. 1993, MNRAS, 260, 705
- Einasto, J. et al. 1997a, Nature, 385, 139
- Einasto, M., Tago, E., Jaaniste, J., Einasto, J., & Andernach, H. 1997b, A&AS, 123, 119
- Einasto, J. et al. 1999, ApJ, in press (astro-ph: 9812247)
- Eisenstein, D.J., Hu, W., Silk, J., Szalay, A.S. 1998, ApJ, 494, L1
- Eke, V. R., Cole, S., & Frenk, C. S. 1996, MNRAS, 282, 263
- Gramann, M. 1988, MNRAS, 234, 569
- Kaiser, N. 1984, ApJ, 284, L9
- Kaiser, N. 1987, MNRAS, 227, 1
- Kashlinsky, A. 1987, ApJ, 317, 19
- Kashlinsky, A. 1998, ApJ, 492, 1
- Klypin, A. A., & Kopylov, A. I. 1983, Soviet. Astron. Lett., 9, 41

- Lacey, C., & Cole, S. 1994, MNRAS, 271, 676
- Landy, S.D., Shectman, S.A., Lin, H., Kirshner, R.P., Oemler, A., Tucker, D., & Schechter, P.L. 1996, ApJ, 456, L1
- Lesgourgues, J., Polarski, D., Starobinsky, A.A., 1998, MNRAS, 297, 769
- Mann, R.G., Heavens, A. F., & Peacock, J. A., 1993, MNRAS, 263, 798
- Mo, H. J., Jing, Y. P., & White, S. D. M., 1996, MNRAS, 282, 1096
- Mo, H. J., & White, S. D. M. 1996, MNRAS, 282, 347 (MW96)
- Peacock, J. A., & Heavens, A. F. 1990, MNRAS, 243, 133
- Peacock, J. A., & Nicholson, D., 1991, MNRAS, 253, 307
- Peacock, J. A., & West, M. 1992, MNRAS, 259, 494
- Postman, M., Huchra, J., & Geller, M. 1992, ApJ, 384, 404
- Press, W. H., & Schechter, P. 1974, ApJ, 187, 425
- Retzlaff, J., Borgani, S., Gottlöber, S., Klypin, A., & Müller, V. 1998, NewA, 3, 631
- Romer, A. K., Collins, C. A., Cruddace R. G., MacGillivray, H., Ebeling, H., Böhringer, H. 1994, Nature, 372, 75
- Starobinsky, A.A., 1992, JETP Lett., 55, 477
- Sugiyama N. 1995, ApJS, 100, 281
- Suhhonenko, I. & Gramann, M. 1999, MNRAS, 303, 77
- Tadros, H., Efstathiou, G., & Dalton, G. B. 1998, MNRAS, 296, 995
- Tammann, G., 1998, in General Relativity, 8th Marcel Crossmann Symposium, ed. T. Piran, (Singapore:World Scientific)
- Tytler, D., Fan, X. M., & Burles, S. 1996, Nature, 381, 207
- White, S. D. M., Efstathiou, G., & Frenk, C. S. 1993, MNRAS, 262, 1023

FIGURE CAPTIONS

Fig. 1.— The power spectrum of the distribution of clusters of galaxies. Open circles show the power spectrum of the distribution of the Abell-ACO clusters and open triangles represent the power spectrum of the APM clusters. Filled circles show the power spectrum of the galaxy distribution in the APM survey.

Fig. 2.— The power spectrum of the distribution of clusters in real space. The heavy lines show the power spectra of clusters determined by approximation (27) and the light lines the corresponding linear power spectra of matter density fluctuations. Panel (a) shows the power spectrum in the model (1) for $\sigma_8 = 0.5$ (dot-dashed lines) and for $\sigma_8 = 0.8$ (solid lines). Open circles and triangles show the power spectra of clusters in N-body simulations for $\sigma_8 = 0.5$ and $\sigma_8 = 0.8$, respectively. Panel (b) shows the power spectrum in the model (2) for $\sigma_8 = 0.5$ (dot-dashed lines) and for $\sigma_8 = 0.84$ (solid lines). Open circles and triangles show the numerical results for $\sigma_8 = 0.5$ and $\sigma_8 = 0.84$, respectively. Error bars in (a) and (b) denote Poisson errors. The power spectrum is shown for the clusters with a mean separation $d_{cl} = 30h^{-1}$ Mpc.

Fig. 3.— The power spectrum of the distribution of clusters in redshift space. Panel (a) shows the results in the model (1) and panel (b) in the model (2). The heavy lines show the power spectra of clusters determined by approximation (29) and the light lines the corresponding linear power spectra of matter fluctuations. Symbols describe the power spectra of clusters in the simulations. In the model (1), we studied clusters for $\sigma_8 = 0.5$, $\Omega = 1$ (dot-dashed lines, open circles), for $\sigma_8 = 0.8$, $\Omega_0 = 0.2$ (dotted lines, crosses) and for $\sigma_8 = 0.8$, $\Omega = 1$ (solid lines, open triangles). In the model (2), clusters were studied for $\sigma_8 = 0.5$, $\Omega = 1$ (dot-dashed lines, open circles), for $\sigma_8 = 0.84$, $\Omega_0 = 0.2$ (dotted lines, crosses) and for $\sigma_8 = 0.84$, $\Omega = 1$ (solid lines, open triangles). The power spectrum is shown for the clusters with a mean separation $d_{cl} = 30h^{-1}$ Mpc.

Fig. 4.— The redshift-space power spectrum of clusters in the Λ CDM models with $\Omega_0 = 0.4$, $h = 0.7$ (solid lines), $\Omega_0 = 0.3$, $h = 0.7$ (dot-dashed lines), $\Omega_0 = 0.4$, $h = 0.5$ (dashed lines) and $\Omega_0 = 0.3$, $h = 0.5$ (dotted lines). The initial spectrum is assumed to be scale-invariant ($P_{in}(k) \propto k$). The heavy lines show the power spectra of clusters determined by approximation (29) and the light lines the corresponding linear power spectra of matter fluctuations. (a) The power spectrum of the model clusters and the Abell-ACO clusters (open circles) with a mean separation $d_{cl} = 34h^{-1}$ Mpc. (b) The power spectrum of the model clusters and the APM clusters (open triangles) with a separation $d_{cl} = 31h^{-1}$ Mpc.

Fig. 5.— The redshift-space power spectrum of clusters in the Λ CDM models with a steplike

initial power spectrum. The heavy lines show the power spectra of clusters determined by approximation (32) and the light lines the corresponding linear power spectra of matter fluctuations. (a) The power spectrum of the model clusters and the Abell-ACO clusters (open circles) with a separation $d_{cl} = 34h^{-1}$ Mpc. We have studied the models with $\Omega_0 = 0.3$, $h = 0.6$, $p = 0.8$ (solid lines) and $\Omega_0 = 0.3$, $h = 0.5$, $p = 0.6$ (dashed lines). The cluster power spectrum is determined for $F = 0.7$. The dot-dashed line shows the cluster power spectrum in the first model for $F = 1.0$. (b) The power spectrum of the model clusters and the APM clusters (open triangles) with a mean separation $d_{cl} = 31h^{-1}$ Mpc. We have studied the model with $\Omega_0 = 0.4$, $h = 0.6$ and $p = 1.25$. The power spectrum of clusters is determined for $F = 0.7$ (solid line) and $F = 1.0$ (dot-dashed line).

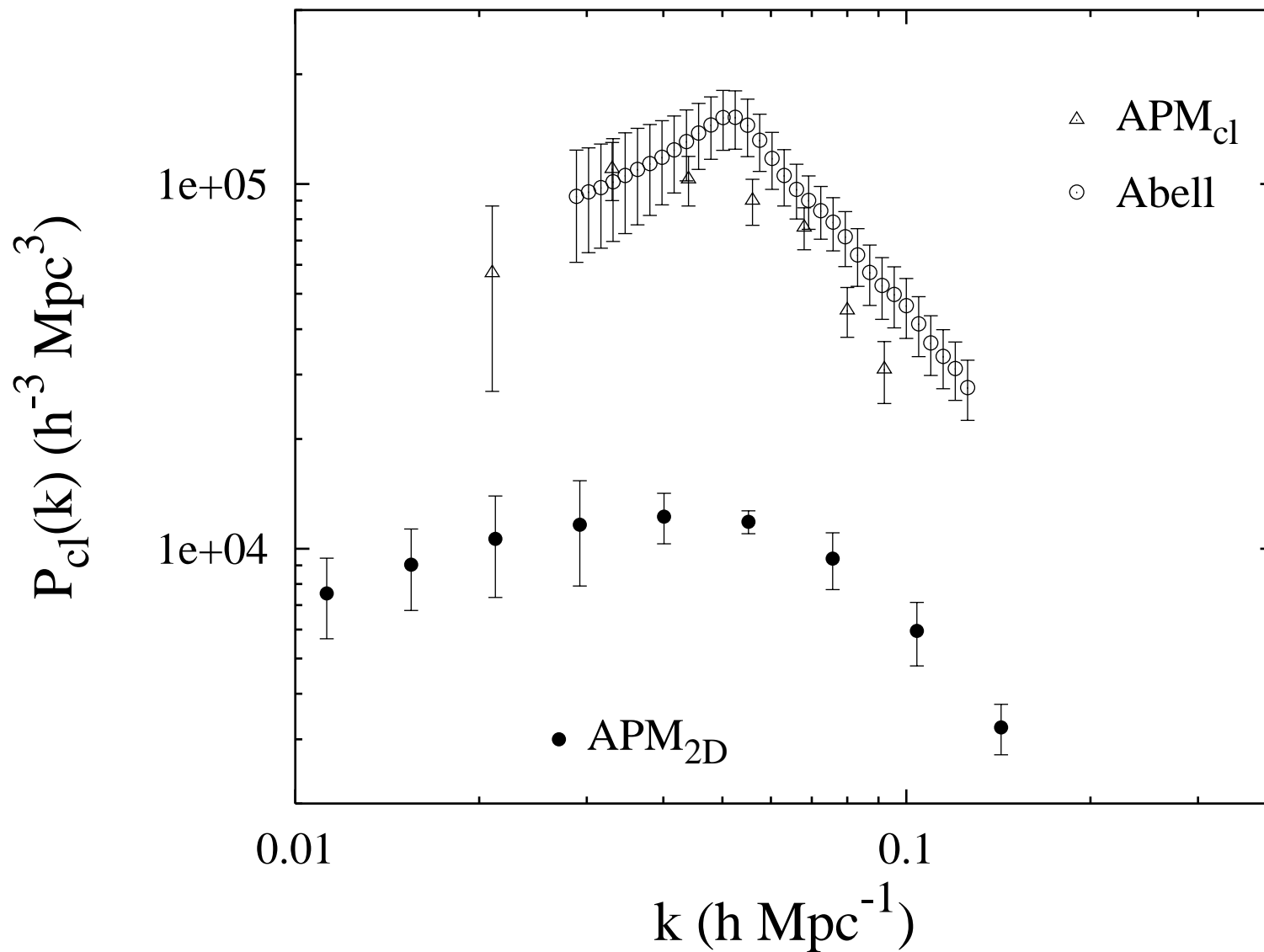


Figure 1

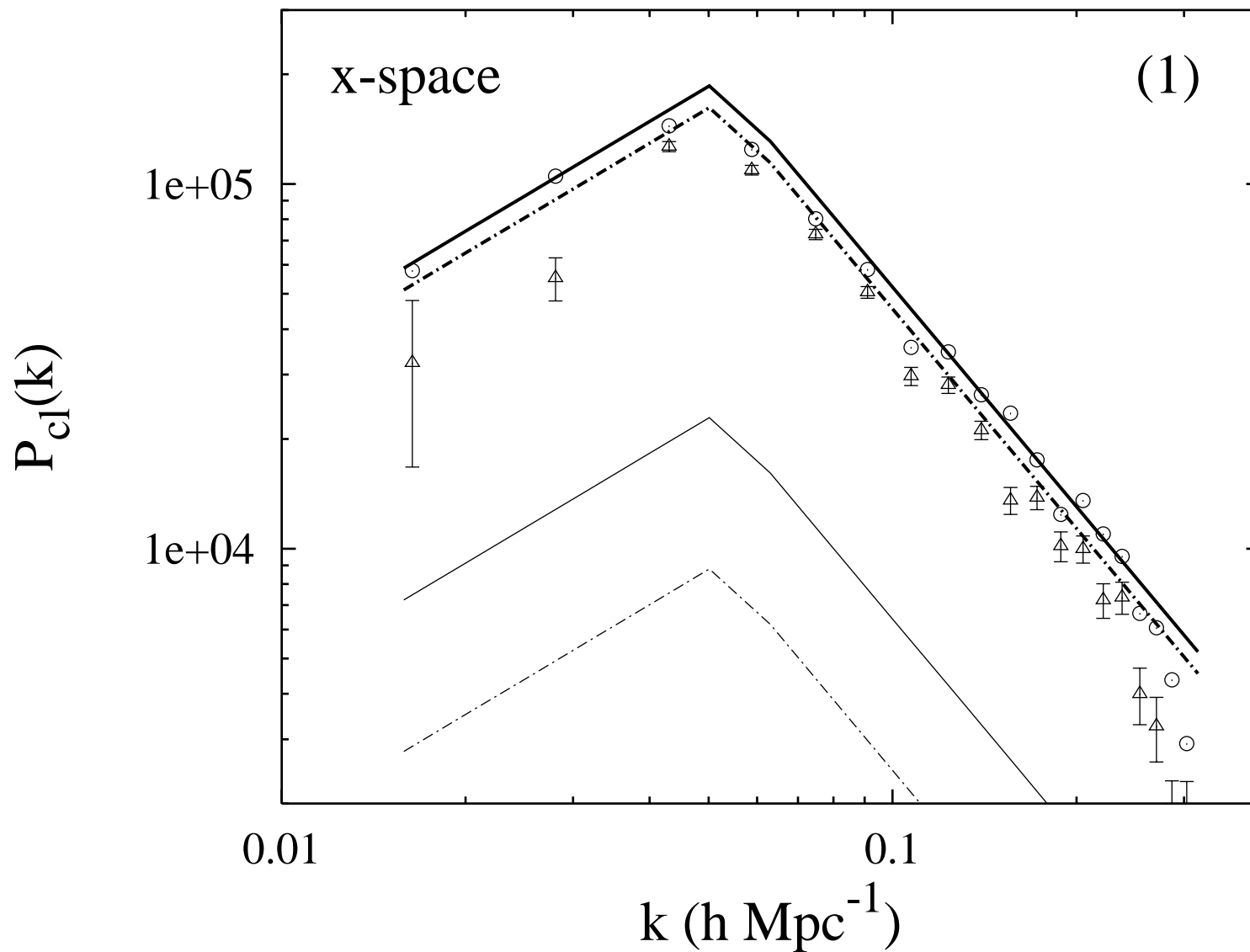


Figure 2a

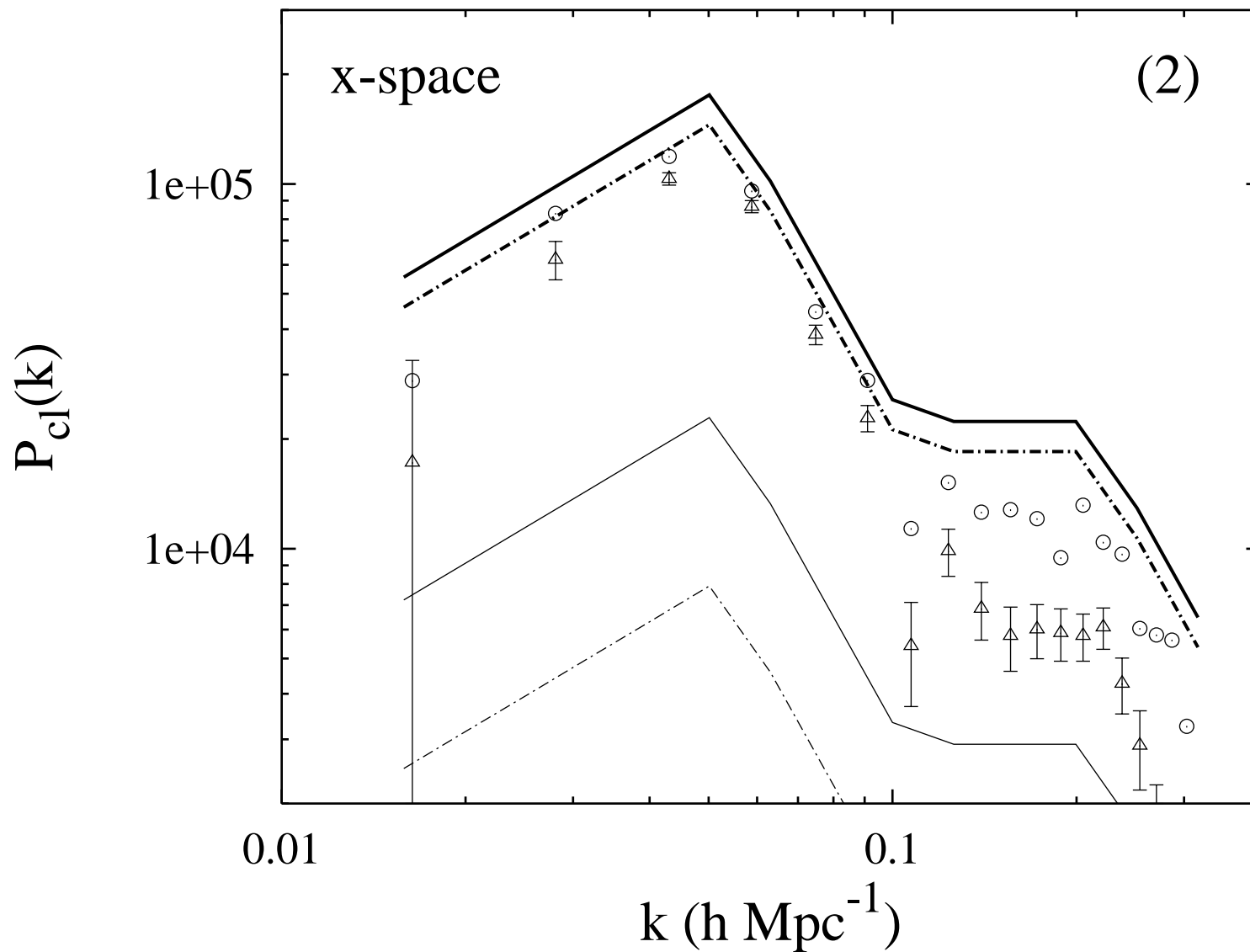


Figure 2b

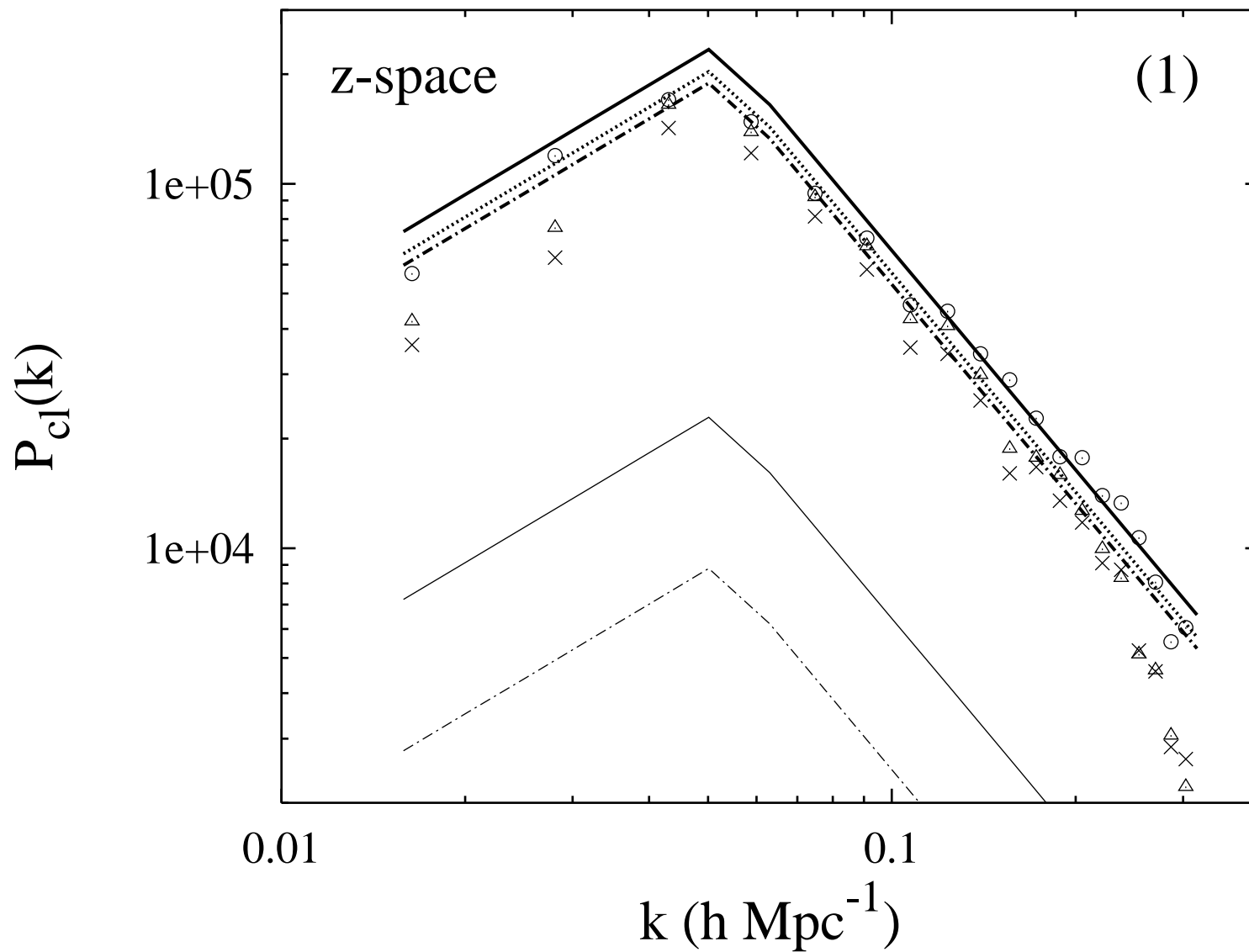


Figure 3a

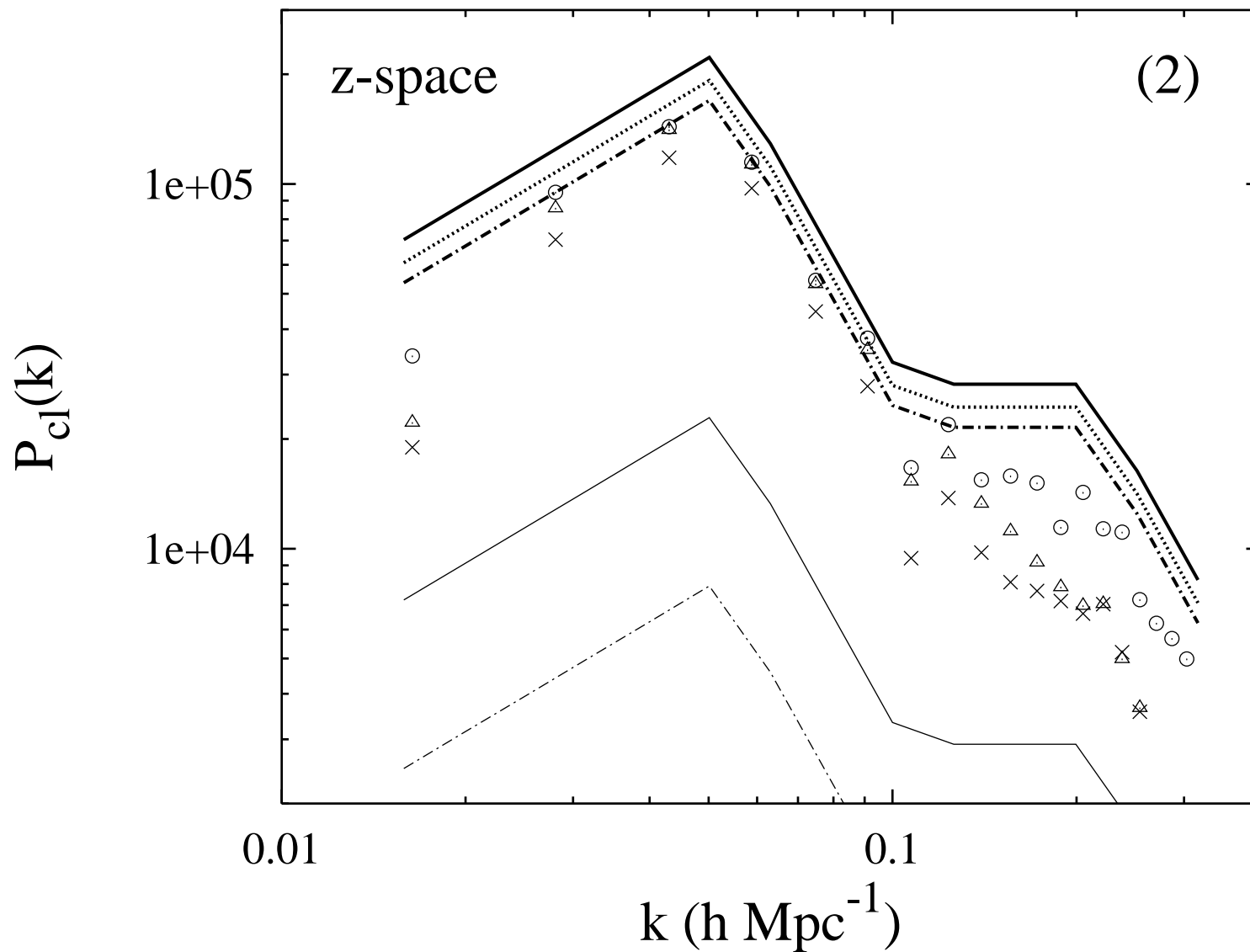


Figure 3b

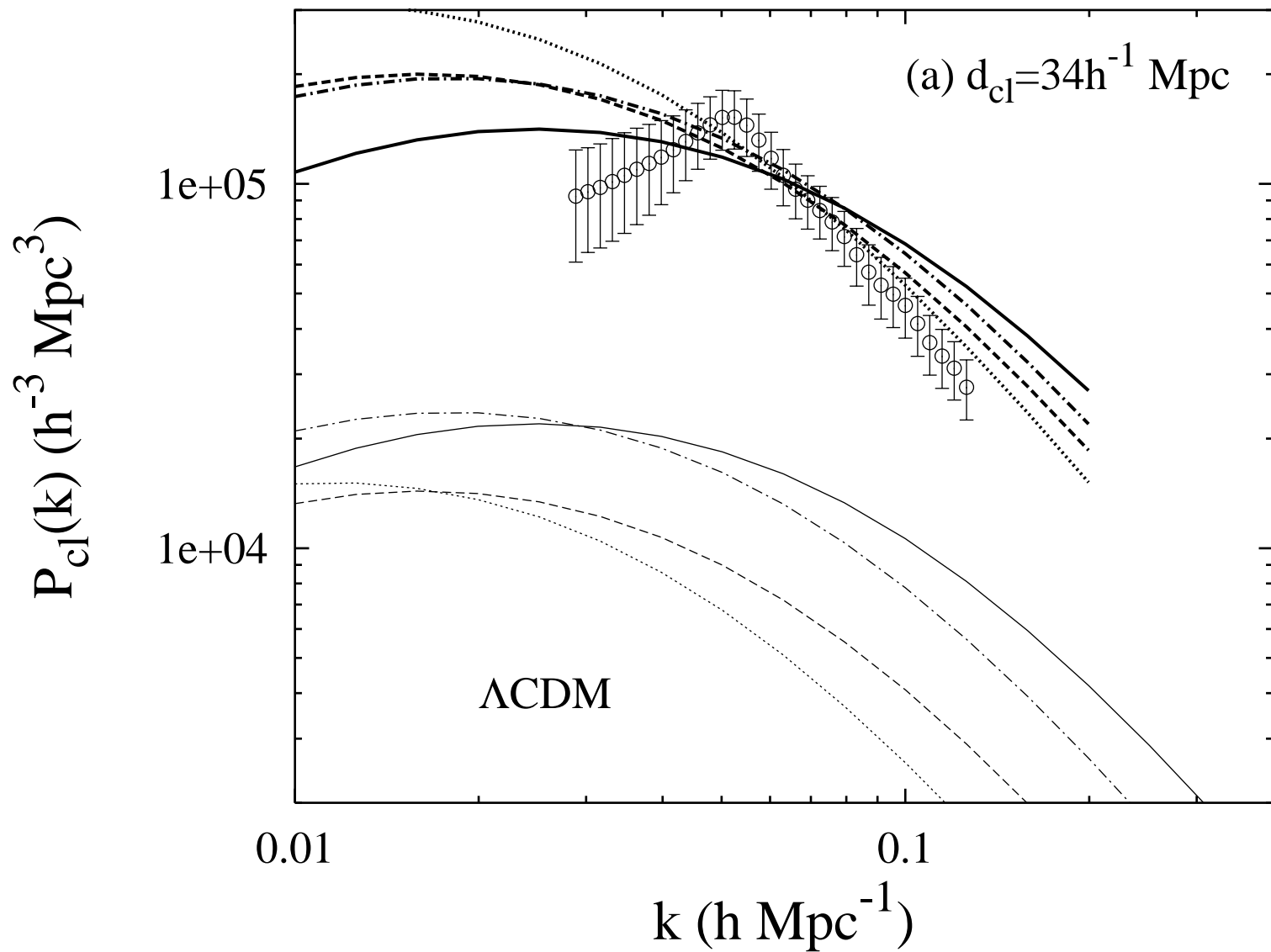


Figure 4a

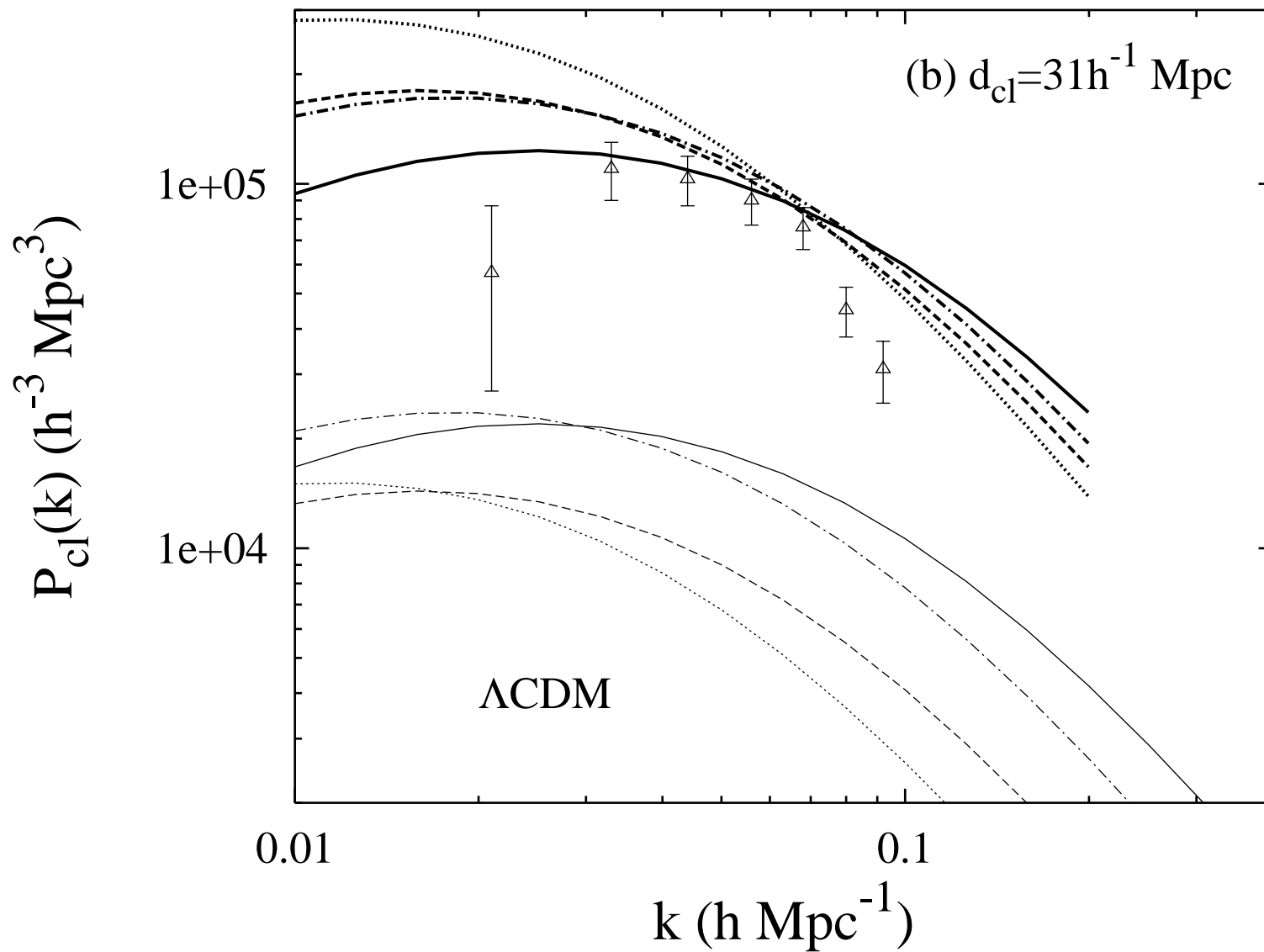


Figure 4b

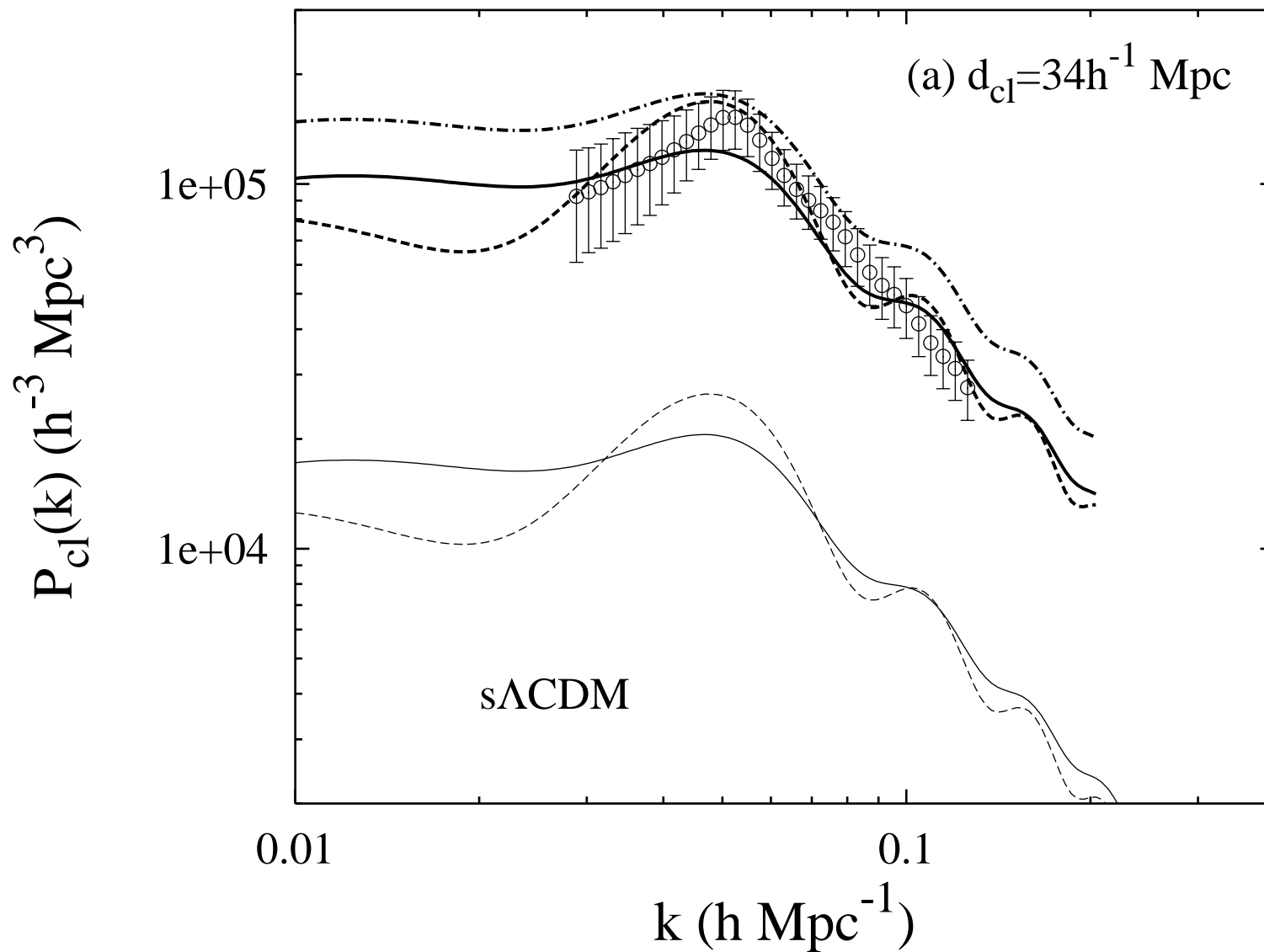


Figure 5a

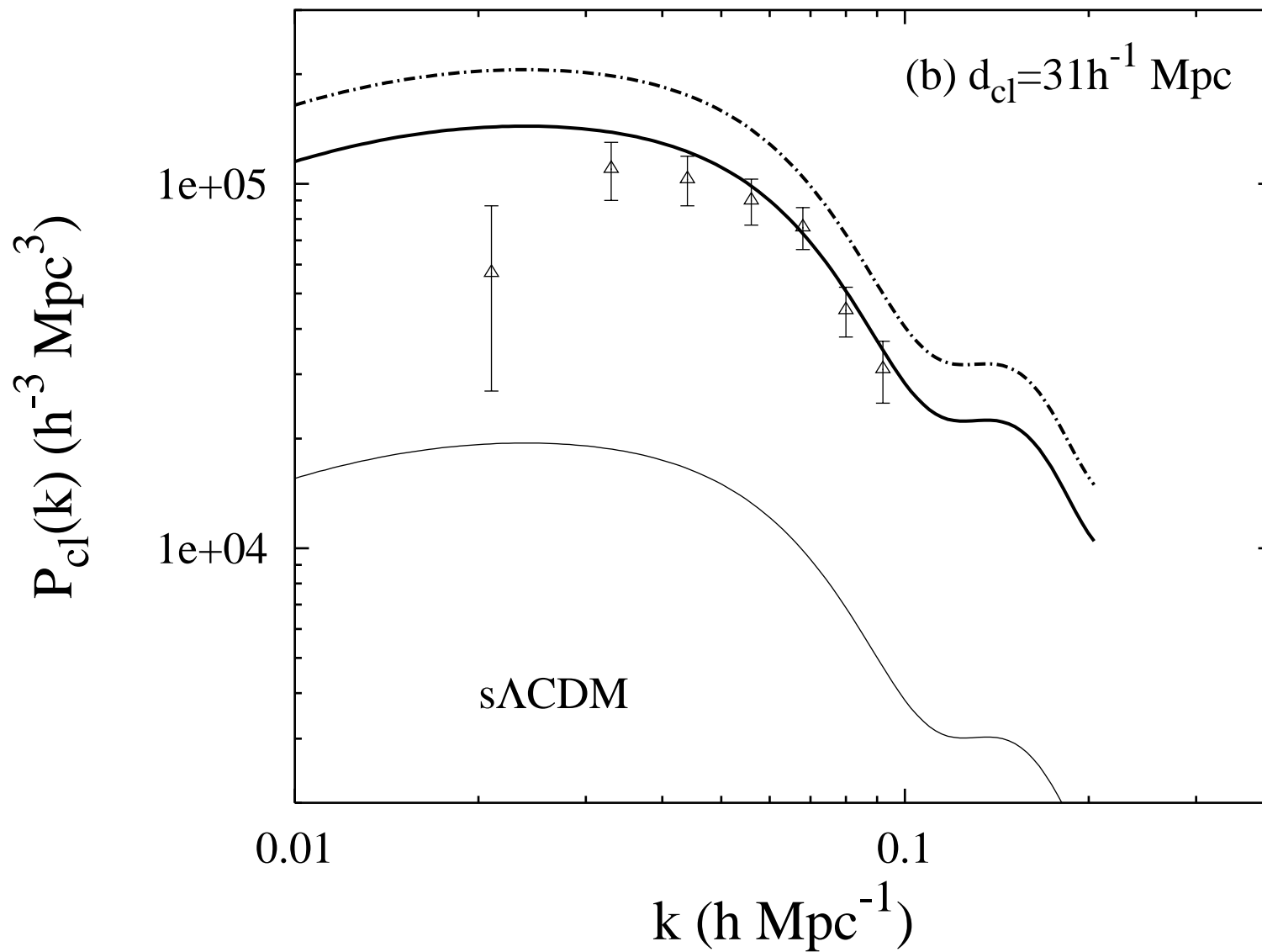


Figure 5b